Contribution from the Department of Chemistry, University of Wyoming, Laramie, Wyoming 82071, and Chemistry Laboratory I, H. C. Ørsted Institute, Universitetsparken 5, DK-2100 Copenhagen Ø, Denmark

Syntheses and Characterization of Binuclear Manganese(III,IV) and -(IV,IV) Complexes with Ligands Related to Tris(2-pyridylmethyl)amine

Aderemi R. Oki,[†] Jørgen Glerup,[‡] and Derek J. Hodgson*,[†]

Received October 11, 1989

The syntheses and spectral, electrochemical, magnetic, and catalytic properties of some new bis(μ-oxo)dimanganese(III,IV) and -(IV,IV) dimers employing a single tetradentate ligand *per* manganese are reported. The crystal structure of $[(L1)Mn-O_2-Mn(L1)](ClO_4)_3\cdot(CH_3CN)$, where L1 is (2-(2-pyridyl)ethyl)bis(2-pyridylmethyl)amine, has been established by X-ray diffraction techniques. The complex, of formula $[Mn_2C_{38}H_{40}N_8O_2]Cl_3O_{12}\cdot CH_3CN$, crystallizes in the triclinic space group $P\bar{1}$ with two independent molecules in a cell of dimensions a = 10.093 (1) Å, b = 12.223 (2) Å, c = 19.625 (2) Å, α = 84.10 (1)°, β = 85.71 (1)°, and γ = 68.468 (9)°. The structure was solved by direct methods and refined by least-squares techniques to a final agreement factor R = 0.0567 based on 6499 independently observed reflections. The complex $[(L3)Mn-O_2-Mn(L3)](ClO_4)_4$, where L3 is ((6-methyl-2-pyridyl)methyl)(2-(2-pyridyl)ethyl)(2-pyridylmethyl)amine, of formula $[Mn_2C_{40}H_{44}N_8O_2](ClO_4)_4$, crystallizes in the monoclinic space group $P2_1/n$ with two molecules in a cell of dimensions a = 12.927 (9) Å, b = 14.277 (7) Å, c = 13.344 (7) Å, and β = 107.62 (5)°. The structure was solved by direct methods and refined to a final value of R = 0.0867 based on 601 observed independent intensities. The magnetic properties of the III/IV complexes are consistent with a doublet ground state, the observed J values being larger (in magnitude) than those for other reported complexes of this type. The IV/IV complex has a singlet ground state, with $2J = -262$ cm^{-1}. The EPR spectra of the III/IV complexes are similar to those observed in related species. The cyclic voltammograms of these and related complexes all show two *quasi*-reversible waves corresponding to III/IV ↔ III/III at 0.219-0.444 V and III/IV ↔ IV/IV at 1.038-1.277 V relative to Ag/AgCl in acetonitrile solvent. These complexes have been shown to preferentially catalyze the epoxidation of cyclohexene using iodosobenzene as the primary oxidant.

Introduction

There has been intense recent interest in the chemistry of binuclear and polynuclear manganese complexes, largely as a result of the importance of high oxidation state manganese species in biological systems; a prime example is photosystem II, in which it is generally believed that four or two manganese atoms are involved in oxygen evolution and that at least two of these manganese atoms occur in a binuclear species with a Mn-Mn separation of about 2.7 Å.[1,2] Our own interest in these types of complexes stems from the observation that binuclear manganese systems have also been shown to catalyze the electrochemical oxidation of alcohols and ethers.[3] The role that manganese plays in all these processes is undoubtedly related to the ability of the metal ions to function as redox catalysts. It is well established that the capacity of metal ions to shuttle between oxidation states can be related to the metal-metal interactions in the clusters as well as to the ligand field around the metal.[4,5] Following the initial report of the synthesis of the binuclear mixed-valent complex $[(bpy)_2MnO]_2^{3+}$ (bpy is 2,2′-bipyridine) and its 1,10-phenanthroline analogue,[6] we[7-10] and others[11-13] have recently examined a number of bis(μ-oxo)dimanganese(III,IV) dimers using tetradentate ligands in place of the bidentate bpy and phen in the hope of reducing the labilities of the various binuclear species which are involved in the IV/IV ↔ III/IV and III/IV ↔ III/III couples. Very recently, we[14] have reported the isolation of a III/III species, and both we and others have characterized IV/IV complexes.[8,15-17] In our recent report on the bis(μ-oxo)dimanganese system with the ligand tris(2-pyridylmethyl)amine (tmpa),[9] we examined the redox potentials of this complex in an attempt to analyze its ability to serve as an electroactive redox catalyst. One goal of our research is to obtain a variety of complexes with a diverse range of redox potentials, so that we can "fine-tune" the potentials for any particular application; our approach here is to chemically modify the ligands so as to bring about desired stereochemical and/or electronic changes at the metal centers. We have, therefore, undertaken a comprehensive study on a series of tetradentate ligands derived from tmpa by slight modification of the steric and electronic environment. We report the syntheses, structural, and spectroscopic characterization of these new complexes, and present comparative catalytic studies on them. The ligands employed are (2-(2-pyridyl)ethyl)bis(2-pyridylmethyl)-amine (L1), (1-(2-pyridyl)ethyl)(2-(2-pyridyl)ethyl)(2-pyridylmethyl)amine (L2), ((6-methyl-2-pyridyl)methyl))(2-(2-pyridyl)ethyl)(2-pyridylmethyl)amine (L3), and ((6-methyl-2-pyridyl)methyl)bis(2-pyridylmethyl)amine (L4).

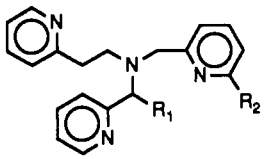

L1: R_1 = H, R_2 = H
L2: R_1 = CH_3, R_2 = H
L3: R_1 = H, R_2 = CH_3

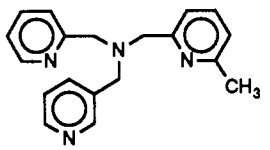

L4

Experimental Section

Syntheses. The ligands were synthesized by slight modifications of previously reported methods.[18,19] All reagents used in these syntheses

[†] University of Wyoming.
[‡] H. C. Ørsted Institute.

(1) Dismukes, G. C. *Photochem. Photobiol.* **1986**, *43*, 99-115.
(2) Yachandra, V. K.; Guiles, R. D.; McDermott, A.; Britt, R.; Dexheimer, S. L.; Sauer, K.; Klein, M. P. *Biochim. Biophys. Acta* **1986**, *850*, 324.
(3) Gref, A.; Balavoine, G.; Rivière, H.; Andrieux, C. P. *Nouv. J. Chim.* **1984**, *8*, 615.
(4) Muetterties, E. L. *Bull. Soc. Chim. Belg.* **1975**, *84*, 959-986.
(5) Buckingham, D. A.; Sargeson, A. M. *Chelating Agents and Metal Chelates*; Dwyer, F. P., Mellor, D. P., Eds.; Academic: New York, 1969.
(6) Nyholm, R. S.; Turco, A. *Chem. Ind. (London)* **1960**, 74.
(7) Collins, M. A.; Hodgson, D. J.; Michelsen, K.; Pedersen, E., *J. Chem. Soc., Chem. Commun.* **1987**, 1659-1660.
(8) Goodson, P. A.; Glerup, J.; Hodgson, D. J.; Michelsen, K., Pedersen, E. *Inorg. Chem.* **1990**, *29*, 503.
(9) Towle, D. K.; Botsford, C. A.; Hodgson, D. J. *Inorg. Chim. Acta* **1988**, *141*, 167-168.
(10) Goodson, P. A.; Hodgson, D. J.; Michelsen, K. *Inorg. Chim. Acta* **1990**, *172*, 49-57.
(11) Hagen, K. S.; Armstrong, W. H.; Hope, H. Inorg. *Chem.* **1988**, *27*, 967-969.
(12) Brewer, K. J.; Liegeois, A.; Otvos, J. W.; Calvin, M.; Spreer, L. O. *J. Chem. Soc., Chem. Commun.* **1988**, 1219-1220.
(13) Suzuki, M.; Senda, H.; Kobayashi, Y.; Oshio, H.; Uehara, A. *Chem. Lett.* **1988**, 1763-1766.
(14) Goodson, P. A.; Hodgson, D. J. *Inorg. Chem.* **1989**, *28*, 3606-3608.
(15) Stebler, M.; Ludi, A.; Bürgi, H.-B. *Inorg. Chem.* **1986**, *25*, 4743-4750.
(16) Suzuki, M.; Tokura, S.; Suhara, M.; Uehara, A. *Chem. Lett.* **1988**, 477-480.
(17) (a) Wieghardt, K.; Bossek, U.; Nuber, B.; Weiss, J.; Bonvoisin, J.; Corbella, M.; Vitols, S. E.; Girerd, J. J. *J. Am. Chem. Soc.* **1988**, *110*, 7398-7411. (b) Libby, E.; Webb, R. J.; Streib, W. E.; Folting, K.; Huffman, J. C.; Hendrickson, D. N.; Christou, G. *Inorg. Chem.* **1989**, *28*, 4037-4040.

0020-1669/90/1329-2435$02.50/0

were purchased from Aldrich Chemical Co. and used without further purification.

(2-(2-Pyridyl)ethyl)bis(2-pyridylmethyl)amine (L1). The ligand was synthesized by reacting 16.4 g (0.1 mol) of 2-picolyl chloride hydrochloride with 6.1 g (0.05 mol) of (2-(2-pyridyl)ethyl)amine in water at room temperature for 5 days, adding 40 mL of 5M aqueous sodium hydroxide solution at intervals to maintain the pH at 8.5–9.0. The resulting dark red solution was extracted with chloroform and the extract dried over sodium sulfate powder. Finally, the chloroform was evaporated under reduced pressure to give a dark brown oil. The pure ligand could be purified by high-vacuum distillation to give a yellow oil. NMR ($CDCl_3$): δ 8.51–7.07 (m, 12 H, aromatic py), 3.92 (s, 4 H, $-CH_2$), 3.06–3.02 (overlapping t, 4 H, J = 2.6 Hz, $-CH_2-CH_2$).

(1-(2-Pyridyl)ethyl)(2-(2-pyridyl)ethyl)(2-pyridylmethyl)amine (L2). 2-Acetylpyridine (0.1 mol) in 50 mL of ethanol was added to (2-(2-pyridyl)ethyl)amine (0.1 mol) in ethanol, and the resulting solution was refluxed for 1 h. A yellow viscous oil remained after removal of the solvent. Sodium borohydride (0.08 mol) was added to the ethanolic solution of this oil, and the mixture was stirred at room temperature for 24 h. Excess hydride was quenched with aqueous HCl, the solution was neutralized, and the product was extracted with chloroform. The solvent was removed by evaporation to leave a yellow oil. This yellow oil (0.07 mol in 20 mL of water) was added to a solution containing 0.07 mol of 2-picolyl chloride hydrochloride; 15 mL of 5 M NaOH was added and a further amount added over a period of 2 days. The resulting dark red solution was extracted with chloroform as above for L1. NMR ($CDCl_3$): δ 8.50–7.00 (m, 12 H, aromatic py), 3.92 (quartet, 1 H, CH, J = 6.0 Hz), 3.88 (s, 2 H, CH_2), 2.95 (overlapping t, 4 H, $-CH_2-CH_2$), 1.48 (d, 3 H, CH_3, J = 6.0 Hz).

((6-Methyl-2-pyridyl)methyl)(2-(2-pyridyl)ethyl)(2-pyridylmethyl)amine (L3). This ligand was prepared as above by using 6-methyl-2-pyridinecarboxaldehyde instead of 2-acetylpyridine. NMR ($CDCl_3$): δ 8.50–6.96 (m, 11 H, aromatic py), 3.89 (s, 4 H, $-CH_2$), 3.00–3.02 (overlapping t, 4 H, J = 6.5 Hz, $-CH_2-CH_2$), 2.51 (s, 3 H, $-CH_3$).

((6-Methyl-2-pyridyl)methyl)bis(2-pyridylmethyl)amine (L4). This ligand was prepared as in L2 by using 6-methyl-2-pyridinecarboxaldehyde and (2-pyridylmethyl)amine instead of 2-acetylpyridine and (2-(2-pyridyl)ethyl)amine, respectively. NMR ($CDCl_3$): δ 8.50–7.14 (m, 11 H, aromatic py), 3.89 (s, 6 H, $-CH_2$), 2.52 (s, 3 H, $-CH_3$).

$[(L1)Mn-O_2-Mn(L1)](ClO_4)_3$ (1). This complex was prepared by mixing an equimolar ratio of aqueous solutions of the ligand (L1) and manganese(II) perchlorate hexahydrate. The resulting solution was stirred for 10 min, and then a few drops of 30% H_2O_2 were added to give a dark green color; a dark green powder deposited after standing for 1 h. Anal. Calcd for $[Mn_2C_{38}H_{40}N_8O_2]Cl_3O_{12}\cdot 3H_2O$: C, 41.38; H, 4.20; N, 10.16. Found:[20a] C, 41.44; H, 3.84; N, 10.04. The product was recrystallized from acetonitrile to give beautifully formed crystals of **1a**, which is an acetonitrile solvate of **1** of formulation $[(L1)Mn-O-Mn(L1)](ClO_4)_3\cdot CH_3CN$.

$[(L3)Mn-O_2-Mn(L3)](ClO_4)_4$ (2). This complex was prepared by chemical oxidation of **4**. The complex (250 mg) is dissolved in a minimum amount of 1 M HCl (about 10 mL); the solution is filtered through filter paper, and 0.5 mL of 10% NaOCl and 0.5 mL 1 M $HClO_4$ are added. The resultant mixture is cooled with ice for 2 h to give dark red crystals of **2**. Yield: 123 mg, 45%. Anal. Calcd for $[Mn_2C_{40}H_{44}N_8O_2]Cl_4O_{16}\cdot 2H_2O$: C, 39.41; H, 3.70; N, 9.22, Cl, 12.06; Mn, 8.72. Found:[20b] C, 39.62; H, 3.99; N, 9.24; Cl, 11.70; Mn, 9.06.

$[(L2)Mn-O_2-Mn(L2)](ClO_4)_3$ (3), $[(L3)Mn-O_2-Mn(L3)](ClO_4)_3$ (4), and $[(L4)Mn-O_2-Mn(L4)](ClO_4)_3$ (5). These complexes are prepared as reported for complex **1**, above, with the appropriate ligand substituted for L1. Anal. Calcd for $[Mn_2C_{40}H_{44}N_8O_2]Cl_3O_{12}\cdot H_2O$ (**3**): C, 43.87; H, 4.23; N, 10.23; Cl, 9.71. Found:[20a] C, 44.11; H, 4.22; N, 10.23; Cl, 9.13. Calcd for $[Mn_2C_{40}H_{44}N_8O_2]Cl_3O_{12}$ (**4**): C, 44.61; H, 4.12; N, 10.40; Cl, 9.87. Found:[20a] C, 45.52; H, 4.32; N, 10.34; Cl, 9.62. Calcd for $[Mn_2C_{38}H_{40}N_8O_2]Cl_3O_{12}$ (**5**): C, 43.51; H, 3.84; N, 10.68; Cl, 10.14. Found:[20a] C, 42.91; H, 3.72; N, 10.76; Cl, 9.43.

Spectroscopy. Electronic absorption spectra were recorded on a Hitachi SPEC 100-80 spectrometer in acetonitrile as solvent. Proton NMR spectra were recorded in $CDCl_3$ on a JEOL FX-270 spectrometer. EPR spectra were recorded at liquid-helium temperature on a Bruker ESP 300 spectrometer operating at a frequency of 9.38 GHz (X-band) with magnetic field modulation of 100 kHz, modulation amplitude of 7 G, and microwave power of 10 mW. Samples were examined as frozen glasses in *N*-methylformamide solution.

Table I. Crystallographic Data for **1a** and **2**

	1a	**2**
formula	$C_{40}H_{43}N_9O_{14}Cl_3Mn_2$	$C_{40}H_{44}N_8O_{18}Cl_4Mn_2$
a, Å	10.093 (1)	12.927 (9)
b, Å	12.223 (2)	14.277 (7)
c, Å	19.625 (2)	13.344 (7)
α, deg	84.10 (1)	90
β, deg	85.71 (1)	107.62 (5)
γ, deg	68.47 (1)	90
V, Å^3	2238.4 (5)	2347 (2)
Z	2	2
fw	1088	1176.5
space group	$P\bar{1}$	$P2_1/n$
T, °C	22	22
μ, mm^{-1}	0.793	0.827
NO[a]	10899	3082
NO [$I > 3\sigma(I)$]	6499	601
R	0.0567	0.0867
R_w	0.0695	0.1239

[a] NO = number of observations.

Magnetochemistry. Magnetic susceptibility measurements were performed by the Faraday method in the temperature range 4–300 K. The molar susceptibilities were corrected for ligand diamagnetism with Pascal's constants.

Electrochemistry. Cyclic voltammetry was performed on a BAS-100A electrochemical analyzer using platinum working electrode. Voltages are reported relative to Ag/AgCl. Solutions were 10^{-3} M in manganese complex in acetonitrile with 0.1 M tetraethylammonium perchlorate as supporting electrolyte.

Catalytic Oxidations of Cyclohexene. Oxidation of cyclohexene was carried out by using iodosobenzene as the primary oxidant. This oxidant was prepared from iodobenzene.[21] The oxidation was performed in acetonitrile, and the products were quantified by GC analysis with a Hewlett-Packard 5890 GC instrument employing a thermal conductivity detector.

X-ray Crystallography. $[(L1)Mn-O_2-Mn(L1)](ClO_4)_3\cdot CH_3CN$ (1a). A powdered sample of **1** was recrystallized from acetonitrile to give a well-formed dark green prism of **1a**. A crystal was mounted on a glass fiber and placed on Nicolet R3m/V diffractometer. Experimental details and cell constants are collected in Table I. The structure was solved by direct methods and refined by full-matrix least-squares techniques. Hydrogen atoms were placed in calculated positions (C–H = 0.96 Å), and all other atoms were refined anisotropically. Final values of the agreement factors are R = 0.0567, R_w = 0.0695. The positional parameters of the non-hydrogen atoms are presented in Table II. Hydrogen atom coordinates, anisotropic librational parameters, and observed and calculated structure amplitudes are available as supplementary material.

$[(L3)Mn-O_2-Mn(L3)](ClO_4)_4$ (2). The Mn(IV)/Mn(IV) complex crystallizes as dark red plates. Data were collected as above, and experimental details are presented in Table I. Regrettably, the crystals diffract very weakly, and very few observable data could be obtained. Consequently, the structure is relatively imprecise (final values of agreement factors are R = 0.0867, R_w = 0.1239), but the general features of the structure are clear and add to our knowledge of the structures of complexes of this general type. Positional parameters of non-hydrogen atoms are presented in Table III. Hydrogen atom coordinates, anisotropic librational parameters, and observed and calculated structure amplitudes are available as supplementary material.

$[(L2)Mn-O_2-Mn(L2)](ClO_4)_3$ (3). The complex crystallized as dark green needles. Unfortunately, the crystals decompose in the X-ray beam, and the structure is poorly determined. The overall features of the structure are very similar to those of **1a**.

All programs used in the structure analyses were from the SHELXTL system as supplied by Nicolet.

Results and Discussion

Structures of the Complexes. $[(L1)Mn-O_2-Mn(L1)](ClO_4)_3\cdot CH_3CN$ (1a). The structure consists of apparently centrosymmetric $[(L1)Mn-O_2-Mn(L1)]^{3+}$ cations, perchlorate anions, and acetonitrile. There are two binuclear manganese cations, having essentially the same structure, in each cell. A view of one of the cations is depicted in Figure 1, and the coordination around the central manganese ions is shown in Figure 2.

(18) Højland, F.; Toftlund, H.; Andersen, S. *Acta Chem. Scand.* **1983**, *A37*, 251–257.
(19) Andregg, G.; Wenk, F. *Helv. Chim. Acta* **1967**, *50*, 2330.
(20) (a) Analyses were performed by Atlantic Microlabs, Norcross, Ga. (b) Analysis performed at H. C. Ørsted Institute.
(21) Lucas, H.; Kennedy, E. R.; Formo, M. W. *Organic Syntheses*; Wiley: New York, 1955; Collect. Vol. III, pp 482–484.

Table II. Atomic Coordinates ($\times 10^4$) and Equivalent Isotropic Displacement Parameters ($Å^2 \times 10^3$) for **1a**

	x	y	z	U(eq)[a]		x	y	z	U(eq)[a]
Mn(1)	132 (1)	4984 (1)	679 (1)	26 (1)	C(4G)	-4158 (9)	11088 (6)	2086 (4)	75 (3)
O(1)	1259 (3)	4829 (3)	-92 (2)	31 (1)	C(5G)	-3231 (9)	10560 (6)	2554 (3)	69 (3)
N(1A)	-479 (4)	6815 (3)	756 (2)	37 (1)	C(6G)	-3772 (6)	10340 (5)	3192 (3)	50 (2)
C(2A)	-1765 (6)	7314 (5)	1038 (3)	48 (2)	C(7G)	-7598 (7)	11340 (6)	3032 (3)	71 (3)
C(3A)	-2345 (8)	8536 (6)	1086 (4)	77 (3)	C(8G)	-7975 (6)	10395 (6)	3436 (3)	59 (3)
C(4A)	-1523 (9)	9200 (6)	840 (4)	78 (3)	N(1H)	-6819 (5)	12004 (4)	4421 (2)	42 (2)
C(5A)	-188 (8)	8662 (6)	574 (3)	67 (3)	C(2H)	-8246 (6)	12299 (4)	4491 (2)	44 (2)
C(6A)	314 (6)	7474 (5)	536 (3)	51 (2)	C(3H)	-9182 (8)	13456 (6)	4476 (3)	67 (3)
C(7A)	-2499 (6)	6460 (5)	1303 (3)	58 (2)	C(4H)	-8628 (13)	14307 (6)	4395 (4)	102 (5)
N(1B)	370 (5)	3210 (4)	983 (2)	49 (2)	C(5H)	-7178 (13)	14054 (7)	4316 (3)	102 (5)
C(2B)	-740 (6)	3113 (5)	1402 (3)	56 (3)	C(6H)	-6269 (9)	12858 (6)	4337 (3)	70 (3)
C(3B)	-771 (10)	2058 (7)	1689 (5)	90 (4)	C(7H)	-8712 (5)	11255 (5)	4569 (3)	44 (2)
C(4B)	251 (15)	1102 (9)	1530 (6)	121 (6)	Cl(1)	-2336 (1)	2935 (1)	3585 (1)	51 (1)
C(5B)	1418 (11)	1052 (7)	1122 (6)	114 (5)	O(1A)	-2669 (7)	3262 (7)	4280 (3)	99 (3)
C(6B)	1491 (8)	2222 (7)	838 (4)	93 (3)	O(1B)	-1788 (8)	1663 (6)	3657 (5)	108 (4)
C(7B)	-1909 (6)	4270 (5)	1543 (3)	56 (2)	O(1C)	-3552 (6)	3403 (6)	3205 (3)	116 (3)
N(1C)	1782 (4)	4726 (3)	1325 (2)	38 (2)	O(1D)	-1251 (9)	3280 (9)	3316 (4)	120 (5)
C(2C)	1676 (9)	4565 (6)	2009 (3)	71 (3)	O(1AA)	-1281 (27)	2261 (23)	3088 (13)	60 (9)
C(3C)	2975 (13)	4325 (7)	2393 (3)	105 (5)	O(1BA)	-2464 (37)	2169 (34)	4061 (18)	77 (10)
C(4C)	4191 (11)	4324 (10)	2004 (6)	127 (6)	O(1DA)	-1704 (44)	3773 (34)	3756 (24)	101 (13)
C(5C)	4248 (9)	4504 (8)	1359 (5)	102 (4)	Cl(2)	-4078 (1)	2319 (1)	32 (1)	54 (1)
C(6C)	3064 (5)	4651 (6)	1042 (3)	61 (3)	O(2A)	-3286 (7)	1522 (5)	-443 (3)	122 (3)
C(7C)	490 (9)	4443 (7)	2364 (3)	83 (4)	O(2B)	-4704 (7)	3448 (5)	-310 (3)	102 (3)
C(8C)	-789 (8)	5349 (6)	2166 (3)	68 (3)	O(2C)	-5154 (7)	1971 (6)	371 (3)	113 (3)
N(1D)	-1345 (4)	5250 (4)	1514 (2)	44 (2)	O(2D)	-3138 (5)	2344 (6)	520 (3)	98 (3)
Mn(2)	-5656 (1)	10183 (1)	4404 (1)	26 (1)	Cl(3)	-4 (2)	2364 (2)	6713 (1)	64 (1)
O(2)	-6046 (3)	9906 (3)	5313 (1)	31 (1)	O(3A)	1238 (11)	2277 (11)	7076 (6)	87 (5)
N(1E)	-5205 (4)	8424 (3)	4195 (2)	39 (2)	O(3B)	-1089 (12)	3433 (7)	6830 (6)	82 (5)
C(2E)	-6342 (6)	8097 (5)	4266 (3)	51 (2)	O(3C)	-414 (12)	1392 (8)	6979 (8)	110 (6)
C(3E)	-6258 (9)	6992 (6)	4141 (4)	91 (4)	O(3D)	316 (20)	2294 (19)	6012 (7)	135 (11)
C(4E)	-4985 (12)	6197 (7)	3950 (5)	111 (5)	O(3AA)	599 (18)	3239 (16)	6553 (11)	130 (10)
C(5E)	-3782 (9)	6502 (6)	3867 (4)	88 (4)	O(3BA)	101 (32)	2073 (23)	7350 (9)	187 (16)
C(6E)	-3928 (6)	7643 (5)	3993 (3)	57 (2)	O(3CA)	-1494 (14)	3050 (16)	6544 (10)	106 (8)
C(7E)	-7717 (5)	9037 (5)	4482 (3)	49 (2)	O(3DA)	567 (21)	1487 (18)	6259 (10)	103 (9)
N(1F)	-7688 (4)	10251 (4)	4181 (2)	44 (2)	C(1)	6180 (11)	2028 (8)	7863 (5)	92 (4)
N(1G)	-5152 (4)	10552 (3)	3372 (2)	38 (1)	C(2)	6775 (18)	2723 (14)	8022 (6)	201 (12)
C(2G)	-6077 (7)	11058 (5)	2878 (3)	60 (2)	N(1)	5529 (14)	1467 (11)	7731 (6)	180 (8)
C(3G)	-5567 (8)	11323 (6)	2199 (3)	71 (3)					

[a] Equivalent isotropic U defined as one-third of the trace of the orthogonalized U_{ij} tensor.

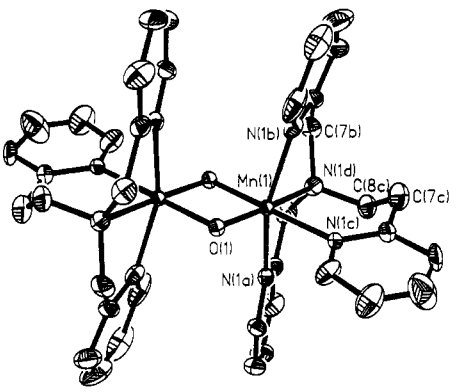

Figure 1. View of the cation in complex **1**. The unlabeled atoms are related to labeled atoms by the inversion operation.

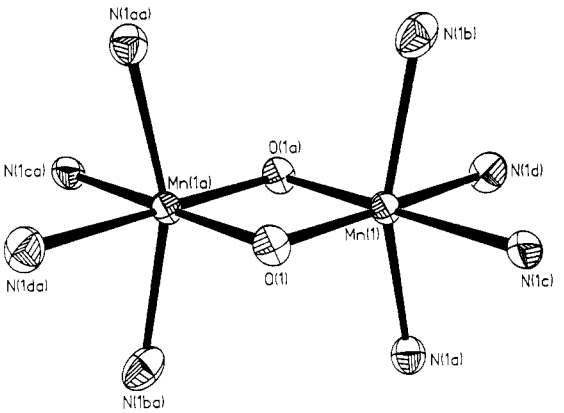

Figure 2. Inner coordination sphere in complex **1**.

The principal bond lengths and bond angles are shown in Tables IV and V, respectively. The Mn–Mn separation of 2.693 (1) Å is considerably longer than the value of 2.643 (1) Å observed in the "parent" tmpa dimer,[9] but is within the range 2.64–2.74 Å reported in a recent tabulation of structures of bis(μ-oxo)dimanganese(III,IV) complexes.[10] The geometry at each manganese center is distorted octahedral, the ligating atoms being the two bridging oxygen atoms and the four nitrogen atoms of the ligand.

Since there is a crystallographic inversion center in the middle of the dimer, the two manganese atoms in the binuclear complex are *crystallographically* equivalent. While this could indicate that the two centers are also *chemically* equivalent, and the odd electron is delocalized around the two manganese centers, a more probable interpretation is the presence of some static or dynamic disorder in the crystals. Static disorder results from the crystallographic superposition of an equal number of Mn(III)–Mn(IV) and Mn(IV)–Mn(III) cations, while dynamic disorder would be caused by rapid (on the crystallographic time scale) electron transfer between the two metal centers. A single crystallographic experiment cannot distinguish between these two forms of disorder but can in suitable cases allow us to distinguish between these disordered models on the one hand and the delocalized model on the other.

A similar situation was reported by Bürgi and co-workers in the analogous phenanthroline binuclear system,[15] where an apparent C_2 symmetry leads to crystallographically equivalent manganese centers and by our own group[10] in the case of two salts of the cyclam analogue; Bürgi and co-workers give an excellent analysis of the crystallographic results associated with disorder. The essential point is that since Mn(III) is a Jahn–Teller ion, it

Table III. Atomic Coordinates ($\times 10^4$) and Equivalent Isotropic Displacement Parameters ($Å^2 \times 10^3$) for **2**

	x	y	z	U(eq)[a]
Mn(1)	778 (6)	346 (5)	4591 (6)	31 (3)
O(1)	251 (24)	-742 (20)	4917 (24)	31 (9)
N(1A)	1954 (32)	459 (28)	5962 (27)	48 (11)
C(1A)	1986 (65)	1159 (54)	6798 (51)	97 (26)
C(2A)	3038 (65)	978 (51)	7716 (58)	130 (24)
C(3A)	3646 (70)	370 (55)	7750 (75)	141 (28)
C(4A)	3780 (70)	-245 (56)	7030 (56)	117 (26)
C(5A)	2784 (45)	-115 (37)	6108 (45)	79 (18)
C(6A)	2698 (54)	-751 (41)	5213 (45)	93 (21)
N(1C)	2056 (39)	-340 (39)	4243 (38)	86 (16)
N(1B)	52 (36)	175 (30)	3061 (34)	67 (14)
C(1B)	-703 (60)	592 (42)	2419 (58)	101 (21)
C(1BA)	-1224 (69)	1330 (56)	2748 (70)	143 (28)
C(2B)	-1287 (71)	324 (52)	1300 (59)	92 (22)
C(3B)	-786 (60)	-388 (52)	1026 (74)	108 (22)
C(4B)	43 (72)	-893 (59)	1566 (68)	125 (27)
C(5B)	507 (50)	-526 (40)	2670 (50)	74 (18)
C(6B)	1426 (51)	-928 (37)	3330 (49)	78 (19)
N(1D)	1232 (35)	1620 (29)	4261 (32)	47 (13)
C(1D)	883 (55)	2355 (36)	4616 (52)	78 (18)
C(2D)	1095 (49)	3351 (41)	4377 (44)	81 (19)
C(3D)	1711 (53)	3392 (53)	3780 (50)	95 (21)
C(4D)	2099 (53)	2690 (42)	3393 (49)	83 (21)
C(5D)	1918 (41)	1750 (31)	3728 (39)	47 (15)
C(6D)	2405 (60)	1030 (45)	3245 (59)	110 (22)
C(7D)	2774 (52)	325 (51)	3901 (54)	96 (19)
Cl(1)	9890 (21)	2860 (15)	634 (19)	82 (12)
Cl(2)	6281 (20)	8603 (17)	-843 (20)	83 (12)
O(2A)	6764 (56)	8058 (36)	38 (49)	166 (35)
O(2B)	5834 (53)	9307 (36)	-505 (51)	189 (40)
O(2C)	5547 (59)	8133 (43)	-1639 (51)	246 (45)
O(1C)	8923 (42)	2967 (30)	866 (33)	109 (25)
O(1D)	9905 (48)	2947 (44)	-329 (47)	169 (41)
O(2D)	6970 (68)	9047 (55)	-1202 (52)	182 (57)
O(1A)	10368 (54)	2030 (51)	976 (52)	202 (46)
O(1B)	10565 (46)	3531 (47)	1136 (38)	161 (36)

[a] Equivalent isotropic U defined as one-third of the trace of the orthogonalized U_{ij} tensor.

Table IV. Selected Bond Lengths (Å) for **1a**

Mn(1)-O(1)	1.806 (4)	Mn(1)-N(1A)	2.111 (5)
Mn(1)-N(1B)	2.118 (5)	Mn(1)-N(1C)	2.081 (5)
Mn(1)-N(1D)	2.098 (5)	Mn(1)-Mn(1A)	2.693 (3)
Mn(1)-O(1A)	1.818 (4)	Mn(2)-O(2)	1.823 (4)
Mn(2)-N(1E)	2.105 (5)	Mn(2)-N(1F)	2.099 (5)
Mn(2)-N(1G)	2.095 (5)	Mn(2)-N(1H)	2.104 (5)
Mn(2)-Mn(2A)	2.691 (3)	Mn(2)-O(2A)	1.807 (4)

Table V. Selected Bond Angles (deg) for **1a**

O(1)-Mn(1)-N(1A)	99.7 (1)	O(1)-Mn(1)-N(1B)	102.0 (2)
N(1A)-Mn(1)-N(1B)	158.0 (2)	O(1)-Mn(1)-N(1C)	94.1 (1)
N(1A)-Mn(1)-N(1C)	88.1 (2)	N(1B)-Mn(1)-N(1C)	86.3 (2)
O(1)-Mn(1)-N(1D)	174.4 (1)	N(1A)-Mn(1)-N(1D)	78.5 (2)
N(1B)-Mn(1)-N(1D)	80.3 (2)	N(1C)-Mn(1)-N(1D)	91.1 (2)
O(1)-Mn(1)-Mn(1A)	42.2 (1)	N(1A)-Mn(1)-Mn(1A)	98.8 (1)
N(1B)-Mn(1)-Mn(1A)	100.0 (1)	N(1C)-Mn(1)-Mn(1A)	136.3 (1)
N(1D)-Mn(1)-Mn(1A)	132.6 (1)	O(1)-Mn(1)-O(1A)	84.0 (1)
N(1A)-Mn(1)-O(1A)	93.4 (2)	N(1B)-Mn(1)-O(1A)	92.9 (2)
N(1C)-Mn(1)-O(1A)	177.8 (1)	N(1D)-Mn(1)-O(1A)	90.9 (2)
Mn(1A)-Mn(1)-O(1A)	41.8 (1)	Mn(1)-O(1)-Mn(1A)	96.0 (1)
Mn(1)-N(1A)-C(2A)	114.2 (4)	Mn(1)-N(1A)-C(6A)	125.6 (3)
O(2)-Mn(2)-N(1E)	93.5 (1)	O(2)-Mn(2)-N(1F)	89.8 (2)
N(1E)-Mn(2)-N(1F)	79.1 (2)	O(2)-Mn(2)-N(1G)	177.1 (2)
N(1E)-Mn(2)-N(1G)	88.6 (2)	N(1F)-Mn(2)-N(1G)	92.5 (2)
O(2)-Mn(2)-N(1H)	92.3 (1)	N(1E)-Mn(2)-N(1H)	157.8 (2)
N(1F)-Mn(2)-N(1H)	79.5 (2)	N(1G)-Mn(2)-N(1H)	86.4 (1)
O(2)-Mn(2)-Mn(2A)	41.9 (1)	N(1E)-Mn(2)-Mn(2A)	99.9 (1)
N(1F)-Mn(2)-Mn(2A)	131.7 (1)	N(1G)-Mn(2)-Mn(2A)	135.8 (1)
N(1H)-Mn(2)-Mn(2A)	98.8 (1)	O(2)-Mn(2)-O(2A)	84.3 (1)
N(1E)-Mn(2)-O(2A)	101.2 (1)	N(1F)-Mn(2)-O(2A)	174.1 (1)
N(1G)-Mn(2)-O(2A)	93.4 (2)	N(1H)-Mn(2)-O(2A)	100.7 (2)
Mn(2A)-Mn(2)-O(2A)	42.4 (1)	Mn(2)-O(2)-Mn(2A)	95.7 (1)

is expected to show elongated axial Mn-N bonds, while the d^3 Mn(IV) center is expected to be approximately spherical; this result is borne out in the structures of all of the Mn(III)/Mn(IV) dimers reported to date. In a disordered structure, therefore, we will see average values for the positions of the axial nitrogen atoms, but since the bond lengths in the two disordered contributors are widely different, there will be large *apparent* thermal motion of the axial nitrogen atoms parallel to the Mn-N bonds. Hence, in a low-temperature X-ray diffraction structure, it is often possible to observe the apparent large thermal motion parallel to the bonds and, hence, to deduce that the system is disordered.[10,15] Regrettably, in a room-temperature diffraction study the effect is masked by the equally large actual thermal motions of the atoms, so (as is evident in Figures 1 and 2, where the ellipsoids representing the eight nitrogen atoms are all approximately the same size and shape) in the present analysis we are unable to demonstrate apodictically the presence of disorder. Obviously, however, the disordered model is the only one that is consistent with earlier observations on related systems. Hence, as has been the case of all bis(μ-oxo)dimanganese(III,IV) complexes, we deduce that in the present complex the two sites are *chemically inequivalent* and that the complex is disordered in the crystal.

As is expected for the disordered system described above, the bridging Mn-O bond lengths of 1.806 (3)-1.823 (3) Å [average value, 1.814 (8) Å] are similar to those of 1.808-1.838 Å found in other disordered systems[10,15] and are intermediate between the average values of 1.776 (8) and 1.837 (3) Å observed for the Mn(IV) and Mn(III) centers, respectively, in the parent tmpa complex.[9] The bridging Mn-O-Mn angles of 95.7 (1) and 96.0 (1)° are within the range 94.0-97.7° reported for other bis(μ-oxo)dimanganese(III,IV) complexes.

As can be seen in Figure 1, the isomer obtained here is the one in which the ethylpyridyl group is equatorial while the two methypyridyl groups are axial. If we compare the N(pyridine)-Mn-N(amine) angles, we observe that while those formed by the five-membered (methylpyridine) rings have angles of 78.5 (2)-80.3 (2)°, the one with the six-membered (ethylpyridine) ring forms an angle of 91.1 (2)°; this may indicate that the observed isomer is favored on steric grounds, since in other isomers the acute angle would be in the equatorial plane.

While one perchlorate is ordered and approximately tetrahedral, with Cl-O distances ranging 1.401 (6) -1.410 (5) Å and angles 109.3(3)-110.2 (4)°, two of the perchlorate ions are highly disordered. One perchlorate ion is disordered around a *pseudo*-3-fold axis defined by the Cl(1)-O(1c) bond. Thus, the two sets of positions O(1aa), O(1ba), O(1da) and O(1a), O(1b), O(1d) are rotated from each other by approximately 60°, with the latter set being 82.4% occupied and the former set 17.6% occupied. This form of disorder has been observed in other recent determinations of perchlorate structures.[22] In the other perchlorate ion all the oxygen atoms are undergoing significant thermal motion around the chlorine, but they have been refined to a model in which there are eight separate oxygen positions, with Cl, O(3a), O(3b), O(3c), O(3d) forming one set of positions with a perfect tetrahedral geometry and occupancy of 57.6% and Cl, O(3aa), O(3ba), O(3ca), O(3da) occupying the other set with 42.4% occupancy.

$[(L2)Mn-O_2-Mn(L2)](ClO_4)_3$ (3). With two molecules in a centrosymmetric triclinic cell, no crystallographic symmetry need be imposed on the cations. In fact, however, the complex crystallizes with two independent cations each having an inversion center in the middle; while this form of packing is unusual, it has been observed in other binuclear complexes.[14,23] The two cations are essentially the same, although the Mn-Mn distances of 2.682 (9) and 2.702 (10) Å are slightly different. A view of one of the cations is shown in Figure 3, and the bond lengths and angles are available as supplementary material. The isomer found here is again the one with the ethylpyridine group in the equatorial position. In view of the imprecision of the metrical parameters, caused by the paucity of data, no further discussion of the structure is warranted.

(22) Hodgson, D. J.; Zietlow, M. H.; Pedersen, E.; Toftlund, H. *Inorg. Chim. Acta* **1988**, *149*, 111-117.
(23) Scaringe, R. P.; Hatfield, W. E.; Hodgson, D. J. *Inorg. Chim. Acta* **1977**, *22*, 175-183.

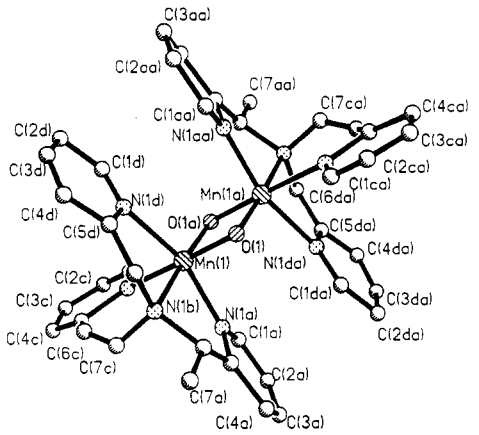

Figure 3. View of the cation in complex **3**.

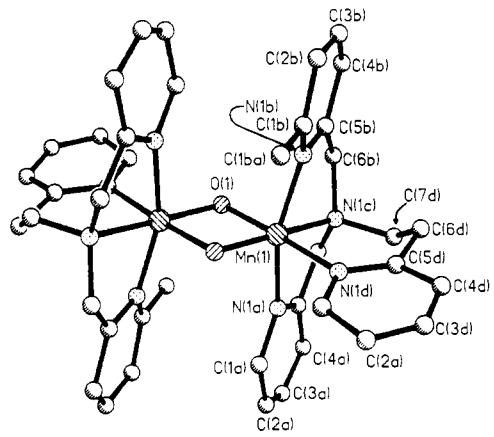

Figure 4. View of the cation in the Mn(IV)/Mn(IV) complex **2**. The unlabeled atoms are related to labeled atoms by the inversion operation.

$[(L3)Mn-O_2-Mn(L3)](ClO_4)_4$ (2). Here again we have very few data because the crystals diffract very poorly, but the structural features of the complex are very clear and add to our presently limited knowledge concerning the structures of Mn(I-V,IV) complexes. The structure of the IV/IV complex consists of $[(L3)Mn-O_2-Mn(L3)]^{4+}$ cations, as shown in Figure 4, and perchlorate anions. The isomer found here is again the one with the ethylpyridine group equatorial, which causes the 6-methylpyridine ring to be axial. The Mn–Mn distance of 2.747 (18) Å is longer than those of 2.643 (1) and 2.693 (1) in the III/IV complexes with the related ligands tmpa[9] and L1 and is slightly outside the range noted earlier for all reported bis(μ-oxo)dimanganese(III,IV) complexes,[10] but is very similar to the value of 2.748 (2) Å reported for the Mn(IV,IV) complex with phen;[15] in the only other structurally characterized bis(μ-oxo)dimanganese(IV,IV) complex, the bispicen analogue, the Mn–Mn separation is only 2.672 (1) Å.[8] Naturally, in the tris(μ-oxo)dimanganese(IV,IV) system recently reported by Wieghardt et al.,[17a] the Mn–Mn separation is much shorter, 2.296 (2) Å. The Mn–O bond lengths of 1.750 (31) and 1.797 (28) Å are apparently shorter than those in the bispicen (1.810–1.812 Å) and phen (1.797–1.805 Å) systems. As is found in the other IV/IV complexes, the average axial Mn–N bond length is 0.05 Å shorter than the average equatorial value, indicating a trans influence of the bridging oxygen atoms on the equatorial nitrogen atoms. The Mn–O–Mn bridging angle of 101.5 (15)° is probably slightly larger than the value of 99.5 (2)° in the phen complex and substantially larger than that of 95.0 (2)° in the bispicen complex.

Electrochemical Properties. A summary of the results of our cyclic voltammetric studies is presented in Table VI. The complexes show two *quasi*-reversible redox waves, whose $E_{1/2}$ values are shown in the table; the peak-to-peak separations range from 70 to 80 mV for the two waves. These potentials represent the III/IV ↔ IV/IV and III/IV ↔ III/III couples. While potentials in this general range have been reported for a variety of mixed-valent binuclear manganese systems,[8] it is noteworthy that substitution in the alkyl arms of the ligands has little effect on the potentials, while substitution at the 6-position of the pyridine group has a major impact. Thus, the potentials of compounds **1** and **3** are similar to each other and to those of the parent tmpa complex, while those for **2** (or **4**) are increased significantly. An even more dramatic demonstration of the same effect was recently reported in the bispicen system, where we demonstrated that the potential for the III ↔ IV couple was increased so much that the III/III form (rather than the III/IV form) was isolated from aqueous solution.[14] As was noted in that earlier report, we attribute this potential shift to steric rather than electronic effects. The crowding caused by the presence of the 6-methyl substituent effectively stabilizes the Mn(III) state, since the axial pyridine group is much further from the metal in the Jahn–Teller-elongated Mn(III) state than in the Mn(IV) state.

Table VI. Cyclic Voltammetric Data for the Complexes

complex	III/III ↔ III/IV[a]	III/IV ↔ IV/IV[a]	complex	III/III ↔ III/IV[a]	III/IV ↔ IV/IV[a]
1a	0.231	1.038	**5**	0.334	1.235
2	0.444	1.277	tmpa	0.245[b]	0.945[b]
3	0.219	1.115		0.285[c]	1.085[c]

[a] Values are in V vs Ag/AgCl. [b] Calculated from data in ref 9, in aqueous medium. [c] Calculated from data in ref 16.

Table VII. Wavelengths (nm) and Extinction Coefficients[a] (M^{-1} cm^{-1}) for the Visible Electronic Spectra

complex	1	2	3
1a	668 (890.8)	557 (902.8)	
2	640 (1394)	538 (1466)	
3	669 (1380)	557 (1520)	
4	675 (1053)	555 (1113)	
5	647 (1062)	559 (1113)	431 (1991)

[a] The number in parentheses is the extinction coefficient.

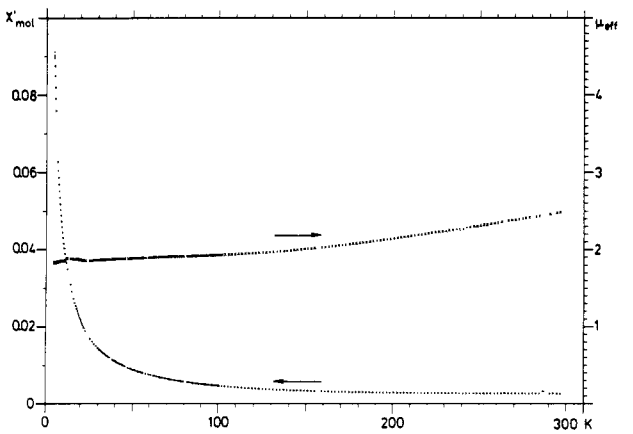

Figure 5. Magnetic susceptibility (left scale) and effective magnetic moment (right scale) of the III/IV complex **4**.

Electronic Spectra. The electronic spectra of the complexes are compared with those of related species in Table VII. In general, two bands were observed in the visible region, at 647–675 nm and at 538–559 nm; a third peak at 431 nm was observed for complex **5**. In the case of the parent tmpa III/IV complex, bands were observed at 443, 561, and 658 nm, and for the IV/IV, analogue the positions were 417, 532, and 641 nm;[16] the similarity of these spectra allow us to assign these visible bands to the Mn^{4+} center and specifically to charge-transfer transitions from the oxo groups to the metal $d\pi^*$ orbitals. We were unable to detect in the spectra of the III/IV complexes the intervalence charge-transfer band that was observed by Cooper and Calvin in the phen system.[24]

(24) Cooper, S. R.; Calvin, M. *J. Am. Chem. Soc.* **1977**, *99*, 6623–6630.

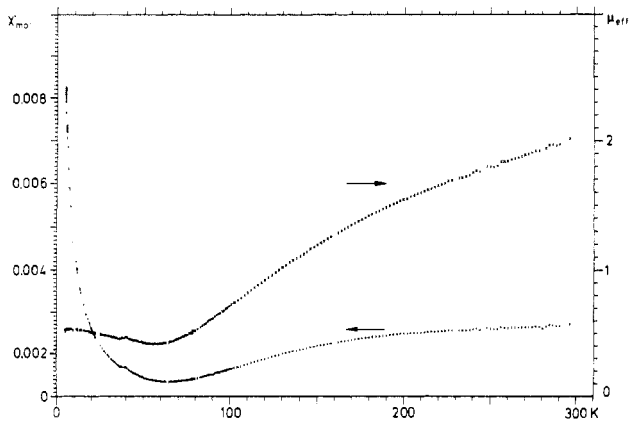

Figure 6. Magnetic susceptibility (left scale) and effective magnetic moment (right scale) of the IV/IV complex **2**.

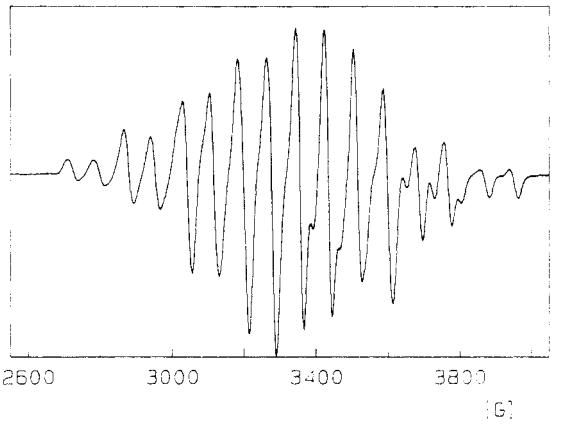

Figure 7. EPR spectrum (4.1 K) of the III/IV complex **4**. The spectra of the complexes **1** and **5** are substantially similar to this but show less anisotropy.

Magnetic Susceptibility. The temperature dependence of the magnetic susceptibility of powdered samples of the mixed-valent III/IV complexes **4** and **5** and of the IV/IV complex **2** were measured in the range 4–296 K. As is shown in Figure 5, for complex **4**, the effective magnetic moment at room temperature is approximately 2.50 μ_B, declining monotonically to a value of 1.81 μ_B at 30 K; the moment is essentially constant below 30 K. The value of 1.81 μ_B corresponds well to the value of $\sqrt{3}\mu_B$ expected for the spin-only moment of a complex with one unpaired electron and indicates that the ground state is a doublet. For complex **5**, the effective magnetic moment declines from 2.8 to 2.4 μ_B in the same temperature range.

The susceptibility data were analyzed by fitting them to the expression

$$\chi'_{mol} = -\frac{N}{H}\frac{\sum_i \frac{\delta E_i}{\delta H}\exp(-E_i/kT)}{\sum_i \exp(-E_i/kT)} + K + \frac{C}{T}$$

where the E_i are the energies of the 20 components of the ground-state manifold. The term C/T accounts for paramagnetic impurities, and K accounts for TIP (temperature-independent paramagnetism) and minor deviations in the correction for the diamagnetic contribution of the atoms. The fitting was accomplished by using the isotropic spin Hamiltonian

$$H = -2J\vec{S}_1\cdot\vec{S}_2 + g_1\beta\vec{S}_1\cdot\vec{H} + g_2\beta\vec{S}_2\cdot\vec{H}$$

where $S = S_1 + S_2$ and we have set $g_1 = g_2$. The Heisenberg term $-2JS_1\cdot S_2$ gives energies of the quartet, sextet, and octet states, relative to the doublet ground state of $-3J$, $-8J$, and $-15J$, respectively. For complex **4**, the fitting leads to a value of $2J = -353 \pm 2$ cm^{-1}. C was found to be 2.7×10^{-2}, which implies approximately 0.3% of a monomeric Mn(II) impurity. For complex **5**, the value of $2J$ was -442 ± 1 cm^{-1} with $C = 3.7 \times 10^{-1}$. These values of $J = -176 \pm 1$ and -221 ± 1 cm^{-1} observed for the mixed-valent complexes here are significantly larger than the values of -150 ± 7, -148 ± 12, -146, -140, and -151 cm^{-1} reported for the bpy,[25] phen,[15] tren,[11] bispicen,[8] and N_3O-py[13] complexes, respectively. In the absence of any structural data for either of these complexes, we cannot ascribe this observed increase in the magnitude of J to any specific structural effect, but it is noteworthy that in related binuclear systems there is a correlation between the magnitude of J and the geometry of the bridging $(MO)_2$ unit.[26,27] The value of $J = -176$ cm^{-1} for **4** means that the complex has a doublet ground state, with the quartet, sextet, and octet states lying at energies of 530, 1412, and 2648 cm^{-1}, respectively, higher than the ground-state doublet. For **5**, the corresponding values are 663, 1768, and 3315 cm^{-1}, respectively.

For the IV/IV complex **2**, as is shown in Figure 6, the effective magnetic moment declines from approximately 2.0 μ_B at room temperature to approximately 0.4 μ_B at 57 K; below 57 K, the effective magnetic moment appears to increase slightly, presumably as the result of the presence of a small quantity of the III/IV complex or of some monomeric material. Similar magnetic properties were observed for the IV/IV complexes of phen[15] and bispicen.[8] The susceptibility data were fitted as above, but since we have two $S = {}^3/_2$ centers in the IV/IV complexes, the Heisenberg term in the Hamiltonian gives rise to a singlet, a triplet, a qiuintet, and a septet state, with energies of 0, $-2J$, $-6J$, and $-12J$, respectively. The fitting leads to a value of $2J = -262.0 \pm 0.9$ cm^{-1}, or $J = -131.0 \pm 0.5$ cm^{-1}. This value of J can be compared to those of -125.6, -137, and -144 cm^{-1} for the bispicen,[8] tmpa,[16] and phen[15] complexes, respectively. Here again, there is no obvious correlation between J and the bridging geometry, but it may be that the geometry of the present complex **2** is insufficiently precisely determined for this purpose.

EPR Spectra. The EPR spectra of the III/IV complexes **1**, **4**, and **5** were measured at 4.1 K; the spectrum of **4**, which exhibits the largest anisotropy, is presented in Figure 7. The spectrum shown in Figure 7 consists of 16 lines. The EPR spectrum was interpreted by means of the hyperfine term[8]

$$A_1\vec{S}_1\cdot\vec{I}_1 + A_2\vec{S}_2\cdot\vec{I}_2$$

in the spin Hamiltonian (where the hyperfine coupling constants are the normal local constants) with $S_1 = 2$, $S_2 = {}^3/_2$, and equal hyperfine constants $A_1 = A_2$. This Hamiltonian leads to a spectrum that should consist of 16 equally spaced lines with the intensity pattern 1,1,2,2,3,3,3,3,3,3,3,3,2,2,1,1. This is, of course, consistent with the result observed in Figure 7. The center of the spectrum corresponds to $g = 2.00 \pm 0.01$.

The observed spectrum comes exclusively from the doublet ($S = {}^1/_2$) ground state. The spacing between adjacent lines is equal to A, the hyperfine coupling constant, the pattern being centered around $(2g_1 - g_2)$. Hence, the present spectrum gives a value of $A = 76 \pm 2$ G. The spectrum reported here is similar to those reported for the phen and bpy complexes[25] and to those of related species. The spectrum of **4** shown in Figure 7 shows the slight anisotropy seen in the phen and bpy spectra, but (as is the case in the bispicen complex[8]) the spectra of **1** and **5** do not.

Epoxidation of Cyclohexene. The epoxidation of cyclohexene by iodosobenzene in the presence of both mononuclear[28-33] and

(25) Cooper, S. R.; Dismukes, G. C.; Klein, M. P.; Calvin, M. *J. Am. Chem. Soc.* **1978**, *100*, 7248–7252.
(26) Crawford, V. H.; Richardson, H. W.; Wasson, J. R.; Hodgson, D. J.; Hatfield, W. E. *Inorg. Chem.* **1976**, *15*, 2107–2110.
(27) Glerup, J.; Hodgson, D. J.; Pedersen, E. *Acta Chem. Scand., Ser. A.* **1983**, *A37*, 161–164.
(28) Dixit, P. S.; Srinivasan, K. *Inorg. Chem.* **1988**, *27*, 4507–4509.
(29) Srinivasan, K.; Michaud, P.; Kochi, J. K. *J. Am. Chem. Soc.* **1986**, *108*, 2309–2320.
(30) Groves, J. T.; Kruper, W. J., Jr.; Haushalter, R. C. *J. Am. Chem. Soc.* **1980**, *102*, 6375–6377.

Table VIII[a]

complex	epoxide formed, mmol	PhI formed, mmol	% epoxide
1	0.02	0.032	62.5
3	0.04	0.066	60.6
4	0.035	0.04	87.5

[a] Conditions: 0.01 mmol catalyst, 0.1 mmol iodosobenzene, 0.97 mmol cyclohexene, and 0.2 mmol chlorobenzene as internal standard. Solutions made up to 5 mL with acetonitrile at room temperature, 2–3 h reaction time. Yield based on iodobenzene formed.

Table IX[a]

	amount, mmol				
complex	catalyst	epoxide	cyclohexenol	PhI	epoxide/catalyst turnover
1	0.0094	0.161	0.040	0.60	17.13
3	0.0102	0.166	0.050	0.422	16.23
4	0.01125	0.255	0.045	0.57	22.60
none	0	0.04	0.02	0.11	

[a] Conditions: 0.81 mmol of iodosobenzene, 3 mmol of cyclohexene, and 0.2 mmol chlorobenzene as internal standard. Solutions made up to 5 mL with acetonitrile at room temperature, 2–3 h reaction time. Yield based on iodobenzene formed. In the absence of catalyst, after 20 h of reaction time, 0.036 mmol of epoxide and 0.14 mmol of cyclohexenol were formed.

binuclear[34] transition-metal complexes has been the subject of intense research activity. In the case of the mononuclear manganese(III) species, the mechanism for this oxidation has been shown to involve the transfer of an oxygen atom from iodosobenzene (or other oxygen donor) to the metal forming an oxomanganese(V) complex; this Mn(V) species acts as a two-electron donor to the substrate (cyclohexene) to form the epoxide.[28,35] For binuclear copper(II) complexes, the mechanism is less clear,[34] and in the case of the present six-coordinate manganese complexes a mechanism involving the formation of a manganese species with a coordinated oxo group is less probable, since such a reaction would be expected to lead to the dissociation of the dimer.

Comparative data for epoxidation activities of the complexes are given in Tables VIII and IX. All the complexes showed preferential catalytic activity toward epoxidation of cyclohexene. As can be seen from the table, introduction of a methyl group at the 6-position on the pyridyl ring causes a significant increase in the yield of epoxide formed. While no concrete mechanism for the catalyzed oxidation by these binuclear complexes has been established, we believe it involves shuttling of the oxidation states in the manganese centers. We observed no significant loss in quantity of manganese complex after the catalytic process. The rate of epoxidation decreases with time, which might be due to some competing process or further oxidation of the epoxide; the possible existence of some further reaction is also consistent with the large decrease in percentage yield of epoxide (relative to the yield of iodobenzene) observed after the reaction is allowed to proceed for 24 h. It is noteworthy, however, that no such reaction was observed in the presence of catalytic mononuclear manganese species under similar conditions.[28]

Acknowledgment. This work was supported by the donors of the Petroleum Research Fund, administered by the American Chemical Society, through a grant to D.J.H., by the National Science Foundation through Grant No. CHE-8912675 to D.J.H., and by the Scientific Affairs Division, North Atlantic Treaty Organization (NATO), through Grant No. 85/0790 to D.J.H. and J.G. We are very grateful to Dr. Kirsten Michelsen for experimental assistance.

Supplementary Material Available: Tables S1 and S2 (hydrogen atom parameters for **1a** and **2**, respectively), S3 and S4 (anisotropic thermal parameters for **1a** and **2**, respectively), and S7–S12 (bond lengths and bond angles for complexes **1a**, **2**, and **3**, respectively) (10 pages); Tables S5 and S6 (observed and calculated structure amplitudes for **1a** and **2**, respectively) (50 pages). Ordering information is given on any current masthead page.

(31) Hill, C. L.; Brown, R. B., Jr. *J. Am. Chem. Soc.* **1986**, *108*, 536–538.
(32) Groves, J. T.; Stern, M. K. *J. Am. Chem. Soc.* **1987**, *109*, 3812–3814.
(33) Oki, A. R.; Hodgson, D. J. *Inorg. Chim. Acta* **1990**, *170*, 65–73.
(34) Tai, A. F.; Margerum, L. D.; Valentine, J. S. *J. Am. Chem. Soc.* **1986**, *108*, 5006–5008.
(35) Koola, J. D.; Kochi, J. K. *J. Org. Chem.* **1987**, *52*, 4545–4553.